Int. J. Heat Mass Transfer. Vol. 36, No. 18, pp. 4327–4333, 1993
Printed in Great Britain

0017-9310/93 $6.00 + 0.00

Thermal Taylor dispersion in an insulated circular cylinder—II. Applications

R. P. BATYCKY, D. A. EDWARDS and H. BRENNER†
Department of Chemical Engineering, Massachusetts Institute of Technology, Cambridge, MA 02139, U.S.A.

(*Received* 5 *January* 1993 *and in final form* 16 *June* 1993)

Abstract—The thermal dispersion theory derived in Part I is here applied to convective heat transfer in an externally insulated tube possessing a finite wall thickness. Expressions are derived for the mean axial thermal propagation velocity $\bar{U}^*$ and thermal dispersivity $\bar{\alpha}^*$ of the composite system for both laminar and turbulent flows. For each, the effect of the nonzero wall thickness is such that $\bar{U}^*$ is always *less* than the average fluid velocity $\bar{V}$. In a laminar flow system, $\bar{\alpha}^*$ can either be larger or smaller than the fluid diffusivity α_f, depending upon the thermal properties of the fluid and wall, as well as upon the magnitude of the Peclet number. For turbulent flows, $\bar{\alpha}^*$ can be either larger or smaller than both α_f and the zero wall thickness effective thermal dispersivity, $\bar{\alpha}_0^*$, although now it further depends upon the Prandtl number.

1. INTRODUCTION

CONSIDER the convective–diffusive transport of heat through an insulated circular tube in which a unidirectional laminar or turbulent flow occurs under the influence of a uniform pressure gradient. The adiabatic, zero normal flux thermal boundary condition will be assumed to apply at the *outer* surface of the finite-thickness tube constraining the flow [1; hereafter referred to as Part I]. Since the tube is insulated at its outer, rather than inner surface, heat can be transported axially (as well as radially) by the tube wall. The wall thickness, $R_0 - R_i$, as well as the thermal transport properties of the tube (and the fluid) will be seen to affect both $\bar{U}^*$ and $\bar{\alpha}^*$. Figure 1 shows the geometrical configuration of the system.

2. LAMINAR FLOW

At the microscale, heat is convected locally with the Poiseuille-flow velocity in the fluid domain, and at zero velocity within the tube wall:‡

$$U(R) = \begin{cases} 2\bar{V}[1-(R/R_i)^2], & (0 \leqslant R < R_i) \\ 0 & (R_i \leqslant R < R_0), \end{cases} \quad (1)$$

with $\bar{V}$ the mean velocity of the fluid. Insofar as their respective functional dependences upon cross-sectional position R are concerned, the pertinent microscale thermophysical properties will be supposed given by the expressions

$$\rho(R)c(R) = \begin{cases} \rho_f c_f = \text{const.} & (0 \leqslant R < R_i), \\ \rho_w c_w = \text{const.} & (R_i \leqslant R \leqslant R_0) \end{cases} \quad (2)$$

and

$$k(R) = \begin{cases} k_f = \text{const.} & (0 \leqslant R < R_i), \\ k_w = \text{const.} & (R_i \leqslant R \leqslant R_0), \end{cases} \quad (3)$$

where subscripts f and w refer to the fluid and wall domains, respectively. These data are used in subsequent subsections to calculate the macroscale thermophysical coefficients $\overline{\rho c}^*$, $\bar{U}^*$ and $\bar{\alpha}^*$ appearing in the macrotransport equation (I-111).§

2.1. *Calculation of* $\overline{\rho c}^*$

Substitution of (2) into (I-115) yields, upon integration over R and ϕ using the piecewise-continuous constancy of ρc within the appropriate regions,

$$\overline{\rho c}^* = \phi_f \rho_f c_f + \phi_w \rho_w c_w, \quad (4)$$

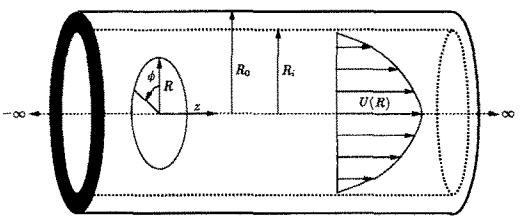

FIG. 1. Tube with a finite wall thickness, $R_0 - R_i$. The no-flux boundary condition applies at the *outer* surface, $R = R_0$. The domain of interest insofar as the transport of heat is concerned corresponds to the region $0 \leqslant R < R_0$.

† Address for correspondence: H. Brenner, MIT, Room 66-562, Cambridge, MA 02139, U.S.A.

‡ The corresponding *turbulent* flow case is discussed in Section 3.

§ Reference to equation numbers in Part I of this series will be made henceforth by affixing the prefix I to the appropriate equation of that paper; thus (I-111) refers to equation (111) of Part I.

NOMENCLATURE

B	field defined by equations (I-64)–(I-66)
c	specific heat capacity
D	molecular diffusivity
$\bar{D}^*$	dispersivity
f	velocity deficit
G, H	functions defined in equations (43) and (44)
I_n	constants, $n = 1$–6
k	thermal conductivity
$k(\xi)$	eddy thermal conductivity of fluid
$\bar{k}^C$, $\bar{k}^M$	respective convective and molecular (i.e. quiescent) contributions to $\bar{k}^*$
$\bar{k}^*$	effective macroscale thermal conductivity
P	pressure
Pe	thermal Peclet number, $\bar{V}R_i/\alpha_f$
Pe_D	material Peclet number, $\bar{V}R_i/D$
Pr	Prandtl number
R	radial coordinate in circular cylindrical coordinate system
R_i, R_0	inner, outer radius of the cylinder
Re_*	Reynolds number based on v_*
Re	Reynolds number, $\bar{V}R_i/\nu$
t	time
U	axial velocity of fluid
U_0	centerline velocity of fluid
$\bar{U}^*$	mean thermal propagation velocity
$\bar{V}$	mean fluid velocity
v_*	friction velocity
z	axial coordinate in circular cylindrical coordinate system.

Greek symbols

α	molecular thermal diffusivity, $k/\rho c$
$\bar{\alpha}^*$	thermal dispersivity
β	volumetric specific heat capacity ratio
γ	thermal conductivity ratio
ν	kinematic viscosity of fluid
ξ	dimensionless radial position, R/R_i
ρ	density
$\overline{\rho c}^*$	macroscale volumetric specific heat capacity
ϕ	angular coordinate in circular cylindrical coordinate system
ϕ_f, ϕ_w	volume fraction of fluid and wall regions, respectively
ω	correction factor for the thermal dispersivity.

Subscripts

f	fluid region
w	wall region.

Superscripts

C	convective contribution
M	molecular contribution.

wherein

$$\phi_f \overset{\text{def}}{=} \left(\frac{R_i}{R_0}\right)^2 \equiv \text{volume and areal fraction of fluid} \tag{5}$$

and $\phi_w = 1 - \phi_f$.

2.2. *Calculation of* $\bar{U}^*$

Substitution of equation (1) together with (2) into (I-113) gives, upon performing the requisite integrations,

$$\bar{U}^* = \frac{\phi_f \rho_f c_f}{\overline{\rho c}^*} \bar{V}. \tag{6}$$

The thermal velocity $\bar{U}^*$ corresponds to the mean velocity at which the 'center of internal energy' is conveyed axially. This velocity clearly obeys the inequality

$$\bar{U}^* \leqslant \bar{V}. \tag{7}$$

Alternatively expressed,

$$\frac{\bar{U}^*}{\bar{V}} = \left(1 + \frac{1-\phi_f}{\phi_f}\beta\right)^{-1}, \tag{8}$$

where we have defined the volumetric specific heat capacity ratio,

$$\beta \overset{\text{def}}{=} \frac{\rho_w c_w}{\rho_f c_f}. \tag{9}$$

The functional dependence of $\bar{U}^*/\bar{V}$ upon ϕ_f and β is displayed generically in Fig. 2, and explicit results for water ($\beta = 0.94$) and a typical oil ($\beta \approx 2.23$) [2, §A.6] flowing through standard steel pipes [3] are given in Table 1. Notice that even for large values of ϕ_f (thin walls), large differences can exist between $\bar{U}^*$ and $\bar{V}$. This is especially true for low heat capacity fluids (e.g. gases) flowing in pipes. Thus, for example, in the case of air flowing through a steel pipe, $\beta \approx 2800$.

2.3. *Calculation of* $\bar{\alpha}^*$

From (I-114), (I-116) and (I-117), the mean conductive contribution

$$\bar{\alpha}^M \overset{\text{def}}{=} \frac{\bar{k}^M}{\overline{\rho c}^*} \tag{10}$$

to the effective thermal dispersivity $\bar{\alpha}^*$ may be obtained from the expression

$$\bar{k}^M = \phi_f k_f + \phi_w k_w. \tag{11}$$

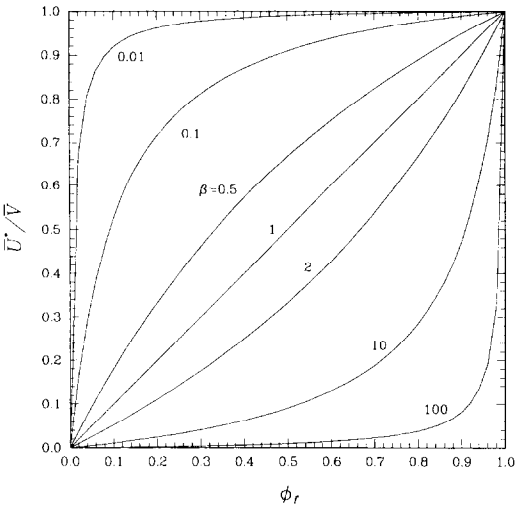

FIG. 2. Average thermal velocity $\bar{U}^*$ relative to average fluid velocity $\bar{V}$ as a function of fluid volume fraction ϕ_f for various specific-heat capacity ratios β.

This corresponds to conductivities in parallel. Expressed in alternative form, these combined expressions may be written as

$$\bar{\alpha}^M = \alpha_f \omega^M, \tag{12}$$

wherein $\alpha_f = k_f/\rho_f c_f$, and ω^M is the dimensionless function

$$\omega^M(\phi_f, \beta, \gamma) = \frac{\phi_f + (1-\phi_f)\gamma}{\phi_f + (1-\phi_f)\beta}, \tag{13}$$

in which

$$\gamma \overset{\text{def}}{=} \frac{k_w}{k_f} \tag{14}$$

is the conductivity ratio. Note that $\omega^M = 1$ when the tube wall is absent, corresponding to $\phi_f = 1$. Figure 3 illustrates the functional dependence explicit in (13).

In order to calculate the convective contribution

$$\bar{\alpha}^C \overset{\text{def}}{=} \frac{\bar{K}^C}{\overline{\rho c}^*} \tag{15}$$

to $\bar{\alpha}^*$ via (I-114), (I-116) and (I-118), one needs first to solve for the B-field, defined by (I-64) to (I-66). Since the forcing function on the right-hand side of (I-64) is a function only of R in the present problem,

Table 1. Thermal velocity $\bar{U}^*$ for water and oil flowing at mean velocity $\bar{V}$ through steel pipes of various sizes

Nominal pipe size (in)	$\bar{U}^*/\bar{V}$	
	Water	Oil
1/8	0.29	0.15
1	0.55	0.36
2	0.68	0.47
12	0.81	0.64

we will assume subject to a posteriori verification that the B-field is of the functional form $B = B(R)$, independent of ϕ. Consequently, equations (I-64) to (I-66) reduce to

$$-\frac{1}{R}\frac{d}{dR}\left(kR\frac{dB}{dR}\right) = \rho c(U - \bar{U}^*), \tag{16}$$

$$\frac{dB}{dR} = 0 \quad \text{at} \quad R = R_0. \tag{17}$$

Use (1) for $U(R)$ in the above, multiply by R, integrate, and subsequently use boundary condition (17) to eventually obtain

$$\frac{dB}{dR} = \begin{cases} \dfrac{\bar{U}^*}{2\alpha_f}\left[\dfrac{\bar{V}}{\bar{U}^* R_i^2}R^3 + \left(1 - \dfrac{2\bar{V}}{\bar{U}^*}\right)R\right] & (0 \leqslant R < R_i), \\ \dfrac{\bar{U}^*}{2\alpha_w}\left(R - \dfrac{R_0^2}{R}\right) & (R_i \leqslant R \leqslant R_0). \end{cases} \tag{18a,b}$$

Requisite quadrature of (I-118) thereby yields

$$\bar{\alpha}^C = \frac{\bar{V} R_i}{48\alpha_f}\omega^C, \tag{19}$$

wherein ω^C is the nondimensional parameter

$$\omega^C(\phi_f, \beta, \gamma) = \frac{\phi_f}{[\phi_f + (1-\phi_f)\beta]^3} \times \left[\phi_f^2 + 6\phi_f(1-\phi_f)\beta + 11(1-\phi_f)^2\beta^2 - 6\frac{\beta^2}{\gamma}\{(1-\phi_f)(3-\phi_f) + 2\ln\phi_f\}\right]. \tag{20}$$

Observe that $\omega^C = 1$ in the absence of the tube wall, namely when $\phi_f \to 1$, in which case (19) reduces to its

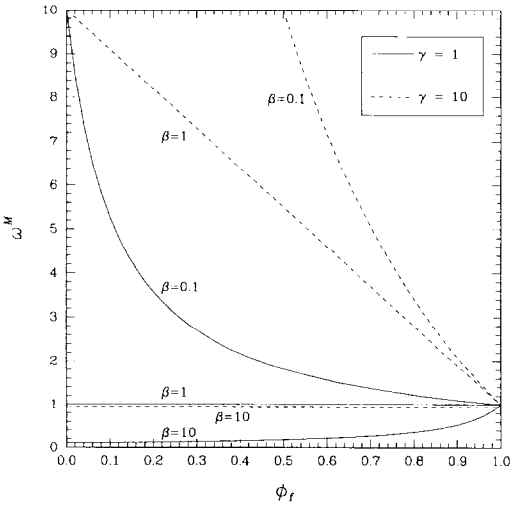

FIG. 3. Dependence of ω^M on ϕ_f for several values of β and γ.

classical Taylor form for material dispersion (where α_f is replaced by the molecular diffusivity D). Figure 4 graphically illustrates the functional dependence explicit in (20).

In combination, the effective thermal dispersivity $\bar{\alpha}^*$ obtained from (12) and (19) adopts the suggestive form

$$\bar{\alpha}^* = \alpha_f\left(\omega^M + \frac{Pe^2}{48}\omega^C\right), \tag{21}$$

where

$$Pe = \frac{\bar{V}R_i}{\alpha_f} \tag{22}$$

is the Peclet number based upon fluid properties. For a vanishingly thin tube wall, where, $\omega^M = \omega^C = 1$, equation (21) reduces to the analog of the comparable Taylor–Aris dispersion formula

$$\bar{D}^* = D\left(1 + \frac{Pe_D^2}{48}\right) \tag{23}$$

for the material Taylor dispersivity $\bar{D}^*$ of a Brownian solute species possessing a molecular diffusivity D (with $Pe_D = \bar{V}R_i/D$).

As shown in Figs. 3 and 4, the functions ω^M and ω^C respectively span the ranges $\omega^M = \omega^C = 1$ at $\phi_f = 1$ to $\omega^M \to \alpha_w/\alpha_f$ and $\omega^C \to 0$ as $\phi_f \to 0$. The latter arises in the absence of a fluid region, corresponding to the case of axial heat conduction through a solid circular cylinder.

Figure 5 displays the dependence of $\bar{\alpha}^*/\alpha_f$ upon ϕ_f and Pe for both oil and water systems (each in a steel tube). Observe how the dispersion increases as the wall thickness increases from zero. Also, note the existence of a volume fraction ϕ_f for which the dispersion is maximized.

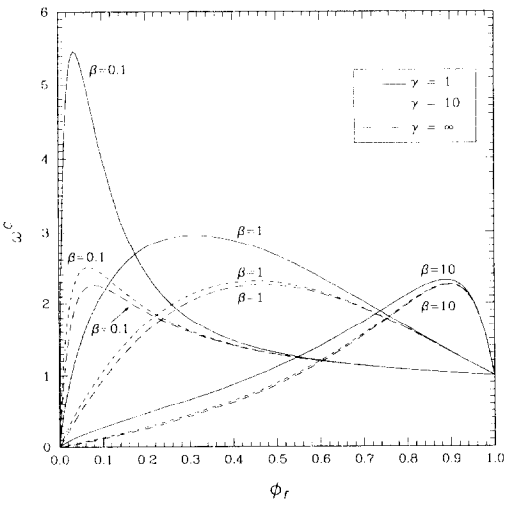

FIG. 4. Dependence of ω^C on ϕ_f for several values of β and γ.

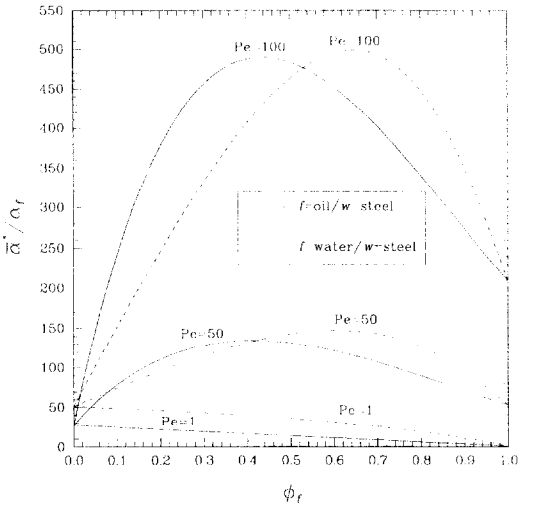

FIG. 5. Effective thermal dispersivity ratio $\bar{\alpha}^*/\alpha_f$ as a function of Peclet number. For oil in a commercial steel tube, $\beta = 2.23$, $\gamma = 114$, whereas for water in a commercial steel tube, $\beta = 0.94$, $\gamma = 25.7$.

2.4. *A limiting case*

Consider the problem wherein the wall thickness goes to zero ($\phi_f \to 1$) while at the same time the heat capacity ratio β tends to infinity such that the following product remains bounded: $(1-\phi_f)\beta = O(1) = \kappa$, say. We also suppose that $(1-\phi_f)\gamma$ and $(1-\phi_f)/\gamma$ are each small compared with unity in the limit $\phi_f \to 1$ (e.g. $\gamma = O(1)$). In this limit, equations (8), (13) and (20) respectively reduce to

$$\frac{\bar{U}^*}{\bar{V}} \to \frac{1}{1+\kappa}, \tag{24}$$

$$\omega^M \to \frac{1}{1+\kappa} \tag{25}$$

and

$$\omega^C \to \frac{1+6\kappa+11\kappa^2}{(1+\kappa)^3}. \tag{26}$$

These formulas correspond to the analogous problem of a Henry's law-type partitioning coefficient occurring during the material dispersion of a solute, such as was originally studied by Golay [4], and later elaborated by Aris [5] and Dill and Brenner [6].

3. TURBULENT FLOW

The generic analysis of Part I applies equally well to the case of turbulent flow as to laminar flow. Turbulent Taylor dispersion was originally discussed by G. I. Taylor [7] for the case of solute dispersion in tubes. In particular, the mean turbulent fluid velocity profile $U(\xi)$ in a circular tube may be expressed as

$$\frac{U_0 - U(\xi)}{v_*} = f(\xi), \tag{27}$$

wherein $\xi = R/R_i$. (Strictly, as in equation (51), $f(\xi)$

also depends functionally upon the friction velocity Reynolds number Re_*, the latter being explicitly defined following equation (28).) Here, U_0 is the centerline velocity of the fluid, v_* the so-called friction velocity, and $f(\xi)$ a universal function, termed the *velocity deficit* [8]. Additionally, Reynold's analogy [8], which simply states that passive contaminants such as heat or matter are transported by turbulent motions in much the same way as momentum, will be assumed to be true. This assumption leads to the conclusion that the eddy thermal conductivity $k(\xi)$ of the fluid is isotropic and varies with radial distance according to the relationship

$$\frac{k(\xi)}{k_f} = \frac{\xi}{f'(\xi)} Pr\, Re_*, \tag{28}$$

in which $f'(\xi) \equiv \mathrm{d}f(\xi)/\mathrm{d}\xi$, $Pr = \nu/\alpha_f$ is the Prandtl number, and $Re_* \overset{\text{def}}{=} R_i v_*/\nu$ is the Reynolds number based on the friction velocity, with ν the kinematic viscosity of the fluid and k_f the thermal conductivity of the quiescent fluid.

It is noteworthy that although we are interested in deriving the macroscale thermal convective–dispersion equations by appropriately averaging the comparable microscale ones, equations (27) and (28) already represent averages over the characteristic length and time scales of the turbulent eddies (instantaneously characterizing the true microscale). Transport phenomena on such fine scales have already been homogenized in producing the apparent steady-state microscale velocity and thermal phenomenological data $U(\xi)$ and $k(\xi)$ appearing in (27) and (28).

For fully-developed flow, a momentum balance yields the following relationship [8] between the axial pressure gradient $\mathrm{d}P/\mathrm{d}z$ in the tube and the friction velocity:

$$v_* = \left(-\frac{R_i}{2\rho_f} \frac{\mathrm{d}P}{\mathrm{d}z} \right)^{1/2}. \tag{29}$$

Furthermore, the relationship between Re_* and the Reynolds number, $Re = R_i \bar{V}/\nu$, can be expressed as

$$Re = \frac{\bar{V}}{v_*} Re_*, \tag{30}$$

which permits Re to be calculated from Re_* via knowledge of $\bar{V}/v_*$ (cf. (33)) and U_0/v_* (cf. (50)).

3.1. *Zero wall thickness*

For the case of a tube with zero wall thickness ($R_i = R_0$), use of (27) and (28) in equations (I-113)–(I-118) yields

$$\overline{\rho c}^* = \rho_f c_f \tag{31}$$

and

$$\bar{U}^* = \bar{V}, \tag{32}$$

with

$$\bar{V} = U_0 - 2v_* I_1 \tag{33}$$

the average fluid velocity, and

$$\bar{\alpha}_0^* = 2(I_2 + I_3) Pr\, Re_* \alpha_f, \tag{34}$$

the effective axial thermal dispersivity for a tube with zero wall thickness. The constants I_1 to I_3 appearing above are respectively defined as

$$I_1 = \int_0^1 f(\xi)\xi \,\mathrm{d}\xi, \tag{35}$$

$$I_2 = \int_0^1 \frac{\xi^2}{f'(\xi)} \mathrm{d}\xi, \tag{36}$$

$$I_3 = \int_0^1 \frac{f'(\xi)}{\xi^2} \left[\int_0^\xi \hat{\xi} f(\hat{\xi})\, \mathrm{d}\hat{\xi} - I_1 \xi^2 \right]^2 \mathrm{d}\xi. \tag{37}$$

Consistent with their physical origins in equation (34), the constant I_2 represents an Aris-like contribution to the effective thermal dispersivity and I_3 a Taylor-like contribution. It will subsequently be seen that $I_2 \ll I_3$ in general.

3.2. *Finite wall thickness*

Similar to the laminar calculations of Section 2, the problem of *turbulent* thermal dispersion in a circular tube having a finite wall thickness will be studied here. Analogous to equations (1)–(3), we write the turbulent axial velocity distribution as

$$U(\xi) = \begin{cases} U_0 - v_* f(\xi) & (0 \leqslant \xi < 1), \\ 0 & (1 \leqslant \xi < R_0/R_i), \end{cases} \tag{38}$$

and the microscale thermophysical properties as

$$\rho(\xi)c(\xi) = \begin{cases} \rho_f c_f = \text{const.} & (0 \leqslant \xi < 1), \\ \rho_w c_w = \text{const.} & (1 \leqslant \xi \leqslant R_0/R_i) \end{cases} \tag{39}$$

and

$$k(\xi) = \begin{cases} \dfrac{\xi}{f'(\xi)} Pr\, Re_* k_f & (0 \leqslant \xi < 1), \\ k_w = \text{const.} & (1 \leqslant \xi \leqslant R_0/R_i). \end{cases} \tag{40}$$

Once again, we are to solve equations (I-113)–(I-118) using equations (38)–(40) so as to obtain the macroscale coefficients $\overline{\rho c}^*$, $\bar{U}^*$ and $\bar{\alpha}^*$.

Equation (4) for the effective volumetric heat capacity continues to apply in present circumstances. Likewise, equation (8) for $\bar{U}^*/\bar{V}$ remains applicable, wherein, as in equation (33), $\bar{V} = U_0 - 2v_* I_1$.

Additionally, the effective thermal dispersivity $\bar{\alpha}^*$ is given by the expression

$$\frac{\bar{\alpha}^*}{\alpha_f} = \frac{2\phi_f G\, Pr\, Re_* - H(\bar{V}/v_*)^2 Pr^2 Re_*^2 + (1-\phi_f)\gamma}{\phi_f + (1-\phi_f)\beta}, \tag{41}$$

or alternatively via (34) as

$$\frac{\bar{\alpha}^*}{\bar{\alpha}_0^*} = \frac{2\phi_f G\, Pr\, Re_* - H(\bar{V}/v_*)^2\, Pr^2\, Re_*^2 + (1-\phi_f)\gamma}{2(I_2+I_3)[\phi_f+(1-\phi_f)\beta]Pr\, Re_*}, \tag{42}$$

wherein

$$G = \frac{1}{4}\left(\frac{U_0}{v_*}\right)^2\left(\frac{\bar{U}^*}{\bar{V}}-1\right)^2 I_4 + \frac{U_0}{v_*}\left(\frac{\bar{U}^*}{\bar{V}}-1\right) \times \left(I_5 - \frac{\bar{U}^*}{\bar{V}} I_1 I_4\right) + I_2 + I_6 - 2\frac{\bar{U}^*}{\bar{V}} I_5 I_1 + \left(\frac{\bar{U}^*}{\bar{V}}\right)^2 I_1^2 I_4, \tag{43}$$

$$H = \frac{\beta^2}{8\phi_f\gamma}\left(\frac{\bar{U}^*}{\bar{V}}\right)^2 [(1-\phi_f)(3-\phi_f)+2\ln\phi_f], \tag{44}$$

and γ is the quiescent thermal conductivity ratio, given by (14). Whereas the nondimensional coefficient G depends upon ϕ_f, β, $f(\xi)$ and U_0/v_*, H depends only upon ϕ_f, β and γ. The numerical constants I_4, I_5 and I_6 appearing above are defined by the expressions

$$I_4 = \int_0^1 \xi^2 f'(\xi)\,d\xi, \tag{45}$$

$$I_5 = \int_0^1 f'(\xi)\left[\int_0^\xi f(\hat{\xi})\hat{\xi}\,d\hat{\xi}\right]d\xi, \tag{46}$$

$$I_6 = \int_0^1 \frac{f'(\xi)}{\xi^2}\left[\int_0^\xi f(\hat{\xi})\hat{\xi}\,d\hat{\xi}\right]^2 d\xi. \tag{47}$$

One may easily confirm equations (41)–(44) in each of the limiting cases $\phi_f \to 0$ and 1, respectively. In the first limit, $\phi_f \to 0$ (corresponding to a solid cylinder composed of the wall material with no fluid region), one correctly obtains $\bar{\alpha}^* \to \alpha_w$. On the other hand, for the zero wall-thickness case, $\phi_f \to 1$, one finds correctly that $\bar{\alpha}^* \to \bar{\alpha}_0^*$ by making use of the identity

$$I_3 = I_6 - 2I_5 I_1 + I_1^2 I_4. \tag{48}$$

As will be seen in the next section, although I_4, I_5 and I_6 may individually depend upon Re_*, the constant I_3 does not.

3.3. *Evaluation of the constants. The velocity deficit law, $f(\xi)$*

In order to numerically implement the quadratures required in the preceding section, and thereby parameterize the results of our analysis, the constants I_1 to I_6 need to be evaluated by first choosing an appropriate empirical functional representation of the velocity deficit $f(\xi)$. For turbulent flow in a tube, the latter may be written as [8]

$$f(\xi) = 1 - 2.5\ln(1-\xi), \tag{49}$$

independently of Re_*. This leads to the logarithmic friction law [8],

$$\frac{U_0}{v_*} = 6 + 2.5\ln Re_*. \tag{50}$$

Equation (49) is based upon scaling arguments valid only in the respective domains where the wall and core regions overlap. It is, however, invalid near the tube center, as well as in the region immediately proximate to the wall. In particular, in the viscous sublayer immediately adjacent to the wall, the velocity actually grows linearly rather than logarithmically with ξ, such that $U \simeq v_* Re_*(1-\xi)$. Hence, with use of (50) the velocity deficit thus becomes

$$f(\xi) = 6 + 2.5\ln Re_* - (1-\xi)\, Re_* \quad (\xi \to 1) \tag{51}$$

near the wall.

An estimate of the point at which the velocity deficit undergoes a transition from linear to logarithmic behavior may be obtained by equating (49) with (51). With ξ_*, say, the intersection point, this immediately gives

$$\xi_* = 1 - \frac{11.0}{Re_*}. \tag{52}$$

The viscous sublayer is thus very thin, and decreases with increasing Reynolds number. Near the center of the tube, a sinusoidal 'wake function' has been proposed [8]. Jointly, the velocity deficit may thus be written as

$$f(\xi) = \begin{cases} 1 - 2.5\ln(1-\xi) - \frac{1}{2}\{\sin[\pi(\frac{1}{2}-\xi)]+1\} \\ \qquad (0 \leqslant \xi < \xi_*), \\ 6 + 2.5\ln Re_* - (1-\xi)\, Re_* \\ \qquad (\xi_* < \zeta \leqslant 1), \end{cases} \tag{53}$$

where ξ_* can be determined from (52).

Use of this velocity deficit function enabled the constants I_1 to I_6 to be computed for various values of Re_*, with results shown in Table 2. The constants I_1, I_2 and I_3, which appear in the theory for the zero wall thickness case, are seen to be insensitive to the Reynolds number. On the other hand, the constants I_4, I_5 and I_6 are strong functions of Reynolds number, with the viscous sublayer playing an important role in determining these constants (even though the combination of these constants is independent of Reynolds number, as in (48)). In his original turbulent dispersion calculation, Taylor [7] disregarded this viscous sublayer contribution, and simply used (49) in the wall region. This was a correct assumption as shown by the insensitivity of the constants I_1 to I_3 to details. However, in our case, with allowance for heat transport into the tube wall, and consequently nonadiabaticity at $\xi = 1$, this sublayer region contributes importantly to the final result. Indeed, were only equation (49) to be used, one would incorrectly conclude that I_4, I_5, $I_6 \to \infty$ at all Reynolds numbers.

Better physical approximations may be made to the velocity deficit. For example, equation (53) shows that $f'(\xi)$ is finite at the center of the tube, when in reality it should be zero. However, since the contribution of this region to $\bar{\alpha}^*$ is small, no need exists for such refinements.

Table 2. Evaluation of the constants I_1 to I_6, and their dependence upon Re_*. (Although I_4, I_5 and I_6 are unbounded at $Re_* = \infty$, their product as defined by (48) remains bounded.)

Re_*	Re	I_1	I_2	I_3	I_4	I_5	I_6
10^3	19×10^3	2.259	0.02780	3.971	18.75	36.97	75.32
10^4	25×10^4	2.230	0.02782	3.641	24.57	50.08	104.8
10^5	30×10^5	2.227	0.02782	3.613	30.33	62.94	133.6
10^6	36×10^6	2.226	0.02782	3.610	36.09	75.77	162.1
∞	∞	2.226	0.02782	3.610	∞	∞	∞

The thermal dispersivity for the zero wall-thickness case is given by (34). Since I_2 and I_3 are approximately independent of Reynolds number, we find that

$$\bar{\alpha}_0^* \simeq 7.27\, Pr\, Re_* \alpha_f. \tag{54}$$

The turbulent thermal dispersivity ratio for a finite wall-thickness is given by (42). For the case of a steel tube, specific results for flowing water and air are given in Figs. 6 and 7. For the turbulent flow of water in a steel tube ($\beta = 0.94$, $\gamma = 25.7$ and $Pr = 7.7$), the general trend is an increase in $\bar{\alpha}^*$ with increasing wall thickness. On the other hand, for a steel tube containing air ($\beta = 2800$, $\gamma = 594$ and $Pr = 0.707$), Fig. 7 shows that the inverse effect is seen, where now $\bar{\alpha}^*$ decreases with increasing wall thickness. Although a bit difficult to ascertain directly from Fig. 7, all curves properly approach unity as $\phi_f \to 1$. (The downturns do not occur until $\phi_f > 0.999$.) Finally, one should be aware of the different scales used in Figs. 6 and 7; specifically, except near the endpoints, the effective thermal dispersivities for the case of water are approximately 3–6 orders of magnitude larger than those for air.

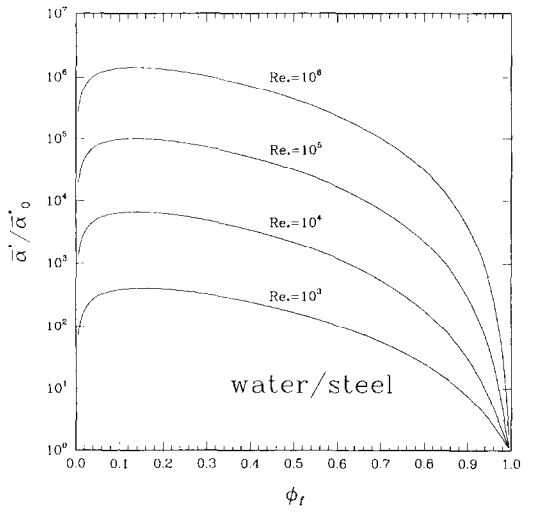

FIG. 6. The ratio of effective thermal dispersivities for the turbulent flow of water in a steel tube with finite wall thickness.

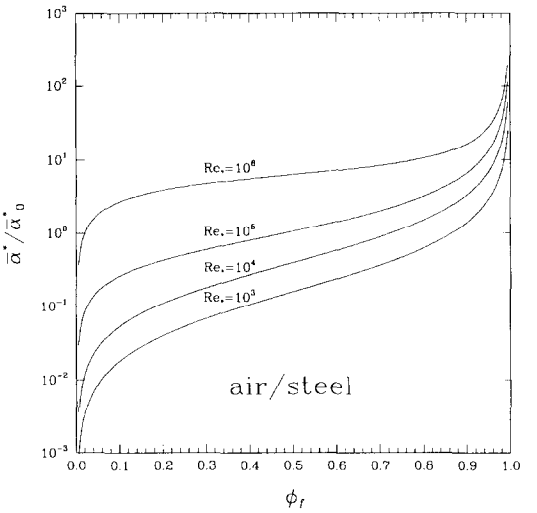

FIG. 7. The ratio of effective thermal dispersivities for the turbulent flow of air in a steel tube with finite wall thickness.

Acknowledgements—This research was supported in part by the Office of Basic Energy Sciences of the Department of Energy.

REFERENCES

1. R. P. Batycky, D. A. Edwards and H. Brenner, Thermal Taylor dispersion in an insulated circular cylinder—I. Theory, *Int. J. Heat Mass Transfer* **36,** 4317–4325 (1993).
2. R. A. Perry and D. W. Green, *Perry's Chemical Engineers' Handbook*. McGraw-Hill, New York (1984).
3. W. L. McCabe, J. C. Smith and P. Harriott, *Unit Operations of Chemical Engineering*. McGraw-Hill, New York (1985).
4. M. J. E. Golay, *Gas Chromatography* (Edited by D. H. Desty), p. 36. Butterworth, London (1958).
5. R. Aris, On the dispersion of a solute by diffusion, convection and exchange between phases, *Proc. R. Soc. Lond. A* **252,** 538–550 (1959).
6. L. H. Dill and H. Brenner, A general theory of Taylor dispersion phenomena—III. Surface transport, *J. Colloid Interface Sci.* **85,** 101–117 (1982).
7. G. I. Taylor, The dispersion of matter in turbulent flow through a pipe, *Proc. R. Soc. Lond. A* **223,** 446–468 (1954).
8. H. Tennekes and J. L. Lumley, *A First Course in Turbulence*. MIT Press, Cambridge (1990).